ORIGINAL CLINICAL REPORT

OPEN

Early Physiologic Numerical and Waveform Characteristics of Simulated Hemorrhagic Events With Healthy Volunteers Donating Blood

Joo Heung Yoon, MD[1]
Jueun Kim, MS[1]
Theodore Lagattuta, RN[2]
Michael R. Pinsky, MD, MCCM[3]
Marilyn Hravnak, RN, PhD[2]
Gilles Clermont, MD, MS[3]

OBJECTIVES: Early signs of bleeding are often masked by the physiologic compensatory responses delaying its identification. We sought to describe early physiologic signatures of bleeding during the blood donation process.

SETTING: Waveform-level vital sign data including electrocardiography, photoplethysmography (PPG), continuous noninvasive arterial pressure, and respiratory waveforms were collected before, during, and after bleeding.

SUBJECTS: Fifty-five healthy volunteers visited blood donation center to donate whole blood.

INTERVENTION: After obtaining the informed consent, 3 minutes of resting time was given to each subject. Then 3 minutes of orthostasis was done, followed by another 3 minutes of resting before the blood donation. After the completion of donating blood, another 3 minutes of postbleeding resting time, followed by 3 minutes of orthostasis period again.

MEASUREMENTS AND MAIN RESULTS: From 55 subjects, waveform signals as well as numerical vital signs (heart rate [HR], respiratory rate, blood pressure) and clinical characteristics were collected, and data from 51 subjects were analyzable. Any adverse events (AEs; dizziness, lightheadedness, nausea) were documented. Statistical and physiologic features including HR variability (HRV) metrics and other waveform morphologic parameters were modeled. Feature trends for all participants across the study protocol were analyzed. No significant changes in HR, blood pressure, or estimated cardiac output were seen during bleeding. Both orthostatic challenges and bleeding significantly decreased time domain and high-frequency domain HRV, and PPG amplitude, whereas increasing PPG amplitude variation. During bleeding, time-domain HRV feature trends were most sensitive to the first 100 mL of blood loss, and incremental changes of different HRV parameters (from 300 mL of blood loss), as well as a PPG morphologic feature (from 400 mL of blood loss), were shown with statistical significance. The AE group ($n = 6$) showed decreased sample entropy compared with the non-AE group during postbleed orthostatic challenge ($p = 0.003$). No significant other trend differences were observed during bleeding between AE and non-AE groups.

CONCLUSIONS: Various HRV-related features were changed during rapid bleeding seen within the first minute. Subjects with AE during postbleeding orthostasis showed decreased sample entropy. These findings could be leveraged toward earlier identification of donors at risk for AE, and more broadly building a data-driven hemorrhage model for the early treatment of critical bleeding.

KEYWORDS: early physiologic signature; heart rate variability; hemorrhage; rapid bleeding

DOI: 10.1097/CCE.0000000000001073

KEY POINTS

Questions: Does very early hemodynamic sign of blood loss exist? Do people who experience adverse events after a small amount of blood loss have characteristic hemodynamic signatures?

Findings: Various waveform or beat-to-beat level features including heart rate variability features changed during small amount of bleeding, with incremental addition of features during blood donation period. Sample entropy was statistically significant for subjects who experienced adverse events after blood donation.

Meanings: Our findings could allow us to develop risk prediction models for the timely detection and management of bleeding patients.

An acute loss of greater than 20% of the total volume of blood causes classic symptoms of hypovolemia while blood loss greater than 40% can be lethal. Blood loss following trauma is the leading cause of death worldwide in ages less than 45 years, and the third contributing cause across all populations (1). Approximately 278,000 people in the United States suffered fatal trauma in 2020 (2), with trauma centers reporting about 37% of inpatient deaths from acute hemorrhagic events (3). It is postulated that 40% of trauma centers' mortalities could be preventable if hemorrhages were detected and treated earlier (4).

The signs of progressive blood loss reflect the effect of reactive increased sympathetic autonomic responses, including increased heart rate (HR) and contractility, with a maintenance of blood pressure (BP) and flow (5). Further volume loss causes selective arterial vasoconstriction and diversion of blood away from visceral organs and the skin to maintain BP, thereby masking hypovolemia. Often arterial pulse pressure (PP) decreases and respiratory rate (RR) increases. With continuing blood loss, these compensatory mechanisms become inadequate to sustain BP and overt hypotensive shock develops. According to the American College of Surgeons Advanced Trauma Life Support (ATLS) classification for hemorrhagic shock, there are observable signs of bleeding before greater than 15% of total blood volume (e.g., 750 mL in a 70-kg subject) is lost (6). However, a hypovolemic threshold has not been proven to reflect real-life hemorrhagic sequelae (7, 8). We hypothesized that the early and easily measurable physiologic changes from noninvasive waveform monitoring of normal volunteer blood donation periods at high bleeding rates could characterize presymptomatic acute volume loss.

MATERIALS AND METHODS

Data Collection

We created a protocol for controlled hemorrhage in human volunteers by collecting continuous noninvasive physiologic multigranular data during blood donation. Periods of orthostasis before and after the blood donation were added to the protocol to mimic clinically significant hemodynamic deterioration. The data were collected from one suburban and one urban donation station managed by a single center (Vitalant, Pittsburgh, PA). Inclusion criteria were age greater than 18 years and donation of a single unit (460–500 mL) of whole blood without IV replenishment. Exclusion criteria were pregnancy, allergy to ECG electrodes, and active infection. The study protocol was approved by the institutional review board for human experimentation at the University of Pittsburgh (IRB MOD19100044-002, September 2, 2020). Blood donation staff directed all arriving donors who expressed interest in hearing about the study to research staff, who then screened for eligibility. We obtained informed consent before conducting study procedures. Procedures were followed in accordance with the ethical standards of the responsible committee on institutional human experimentation and with the Helsinki Declaration of 1975.

Noninvasive waveform-level signals of electrocardiography (ECG, 250 Hz), photoplethysmography (PPG, 125 Hz), continuous noninvasive arterial BP waveforms (continuous noninvasive arterial pressure [CNAP], 100 Hz), and respiratory waveforms (125 Hz) were collected using a portable MP50 monitor (Philips, Amsterdam, The Netherlands), and downloaded onto a study computer using a data collection software (Medicollector, Winchester, MA) (**Fig. 1**). In addition, we obtained participant demographics (age, ethnicity, height, weight, and body mass index) and past medical history (prevalence of hypertension, current medications including antihypertensive medications, history of hypothyroidism, smoking, drinking, history of SARS-CoV-2 (COVID-19),

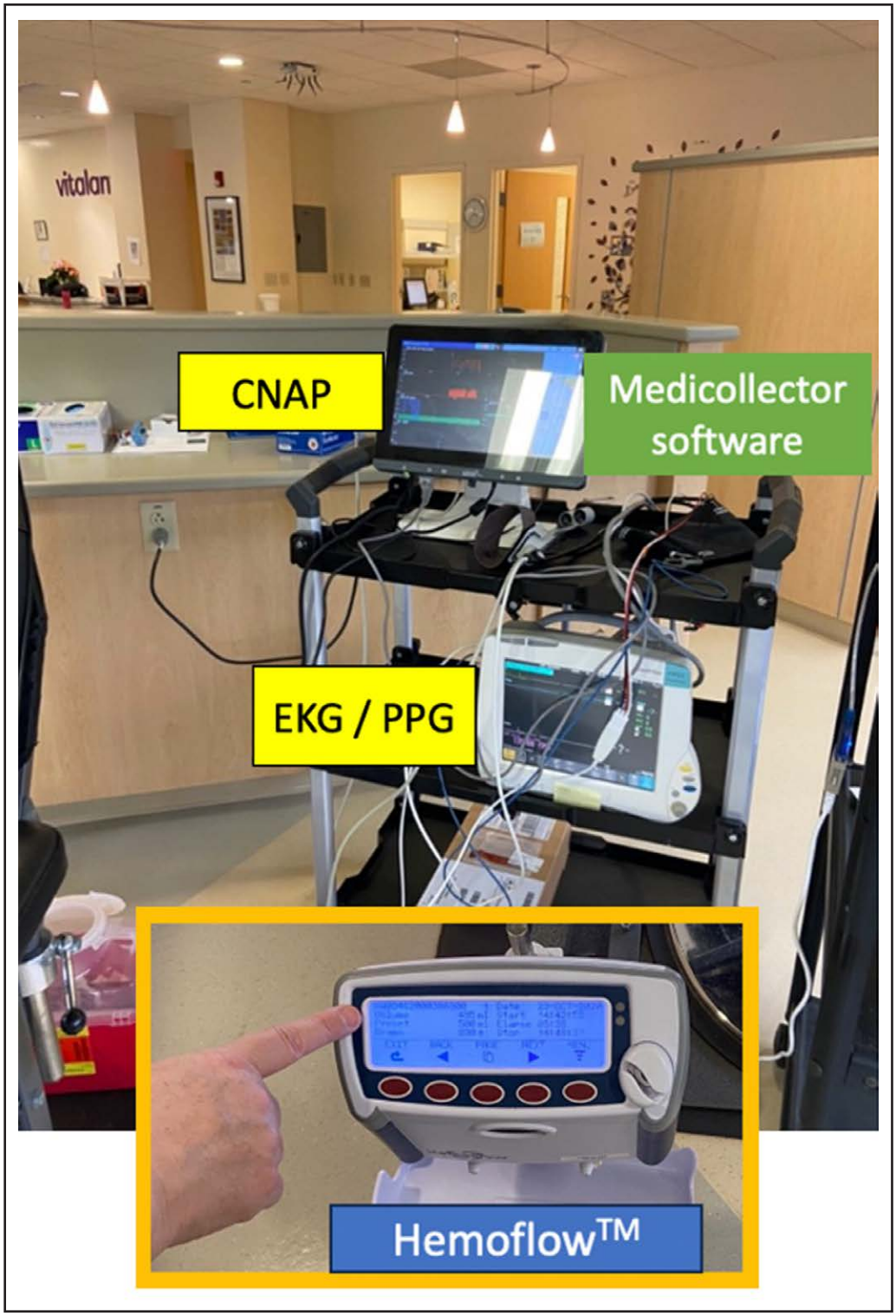

Figure 1. The setup of the physiologic vital sign collection devices. Electrocardiography (ECG) and photoplethysmography (PPG) signals were collected through the Philips MP50 transfer monitor and continuous noninvasive arterial pressure (CNAP) signals were collected via the LiDCO monitor. Raw data collected from both machines were then incorporated into a research laptop computer equipped with waveform-handling software (Medicollector) with annotations for position changes or symptoms of participants during the data collection. Hemoflow device measured the amount of blood volume collected during the blood donation (*orange box*).

prevalence of joint pain/inflammation, and symptoms of joint hypermobility by the Beighton score system [9]).

The data collection protocol was as follows. Briefly, after explaining the protocol steps to the participants, ECG electrodes, a PPG fingertip sensor (Masimo pulse oximeter, Irvine, CA), and finger cuff CNAP (LiDCO rapid monitor, LiDCO, London, United Kingdom) were attached, and the participant was observed for 3 minutes while sitting in the blood donation chair (prebleed baseline). Participants were then asked to stand for 3 minutes (prebleed orthostasis) and sit again. Participants were placed in a blood donation chair in a semi-recumbent position, whereafter venous cannulation was performed by donation staff, a BP cuff placed proximate to the IV site was inflated to 20 mm Hg and bleeding commenced. During blood donation, the bleeding rate was continuously monitored (Hemoflow, Applied Science, Grass Valley, CA). For sequential analysis, we segmented the bleeding into 100 mL episodes with start of bleeding (Fig. 1). After

the blood donation was complete, the participant was observed for 3 minutes in the blood donation chair (postbleed baseline), and again asked to stand for 3 minutes (postbleed orthostasis) (**Fig. 2**).

Adverse events (AEs) such as self-reported dizziness, lightheadedness, nausea, observed facial flush, sweating, and feelings of impending doom at any time during or after bleeding were recorded. Participants were allowed to change to a recumbent position (with or without raising their legs) to minimize further AE. Soft drinks, snacks, and cooling pads were provided as needed by donation center protocol. When the participants with AE were deemed hemodynamically stable and without subsequent AE symptoms, they were asked whether they wanted to continue with blood donation and study participation. If affirmative, the study protocol was continued.

Physiologic Signal Processing Methods

For each vital sign data stream, physiologic variables were computed using different time windows (**Table 1**) and summarized below.

ECG Waveform Processing and Analysis. Lead II or III ECG waveforms were selected for analysis based on the visibility of R wave peaks in the QRS complex. A bandpass filter was applied as a form of notch filter (10) to remove artifactual amplitude and 60 Hz noise. The peak detection algorithm identified R peaks, to produce beat-to-beat HR. Based on the R–R interval time series, HR variability (HRV) metrics were calculated (Matlab and Python software [11]).

For HRV time-domain variables, the SD of interbeat (N-to-N) interval (SDNN) and root mean squared SD of interbeat interval (RMSSD), the SD of successive differences (SDSD), as well as the percentage of successive RR interval greater than or equal to 20 and 50 ms (pNN20, pNN50) were calculated as previously reported (12). For HRV frequency domain processing, the RR interval was computed to estimate the distribution of power in different frequency bands including low frequency (LF, 0.04–0.15 Hz, affected by RR, 4–10/min), high frequency (HF, 0.15–0.40 Hz, affected by RR, 8–25/min), and the ratio of LF to HF (LF/HF ratio) to serve as a reflection of the relationship between the sympathetic and parasympathetic systems. For the nonlinear variable, sample entropy (SampEn), a measure of complexity of the physiologic time series data (13), was calculated from a 2-minute time period, with 1-minute overlapping windows.

PPG Waveform Processing and Analysis. PPG waveform measured from a fingertip oximeter is a complex

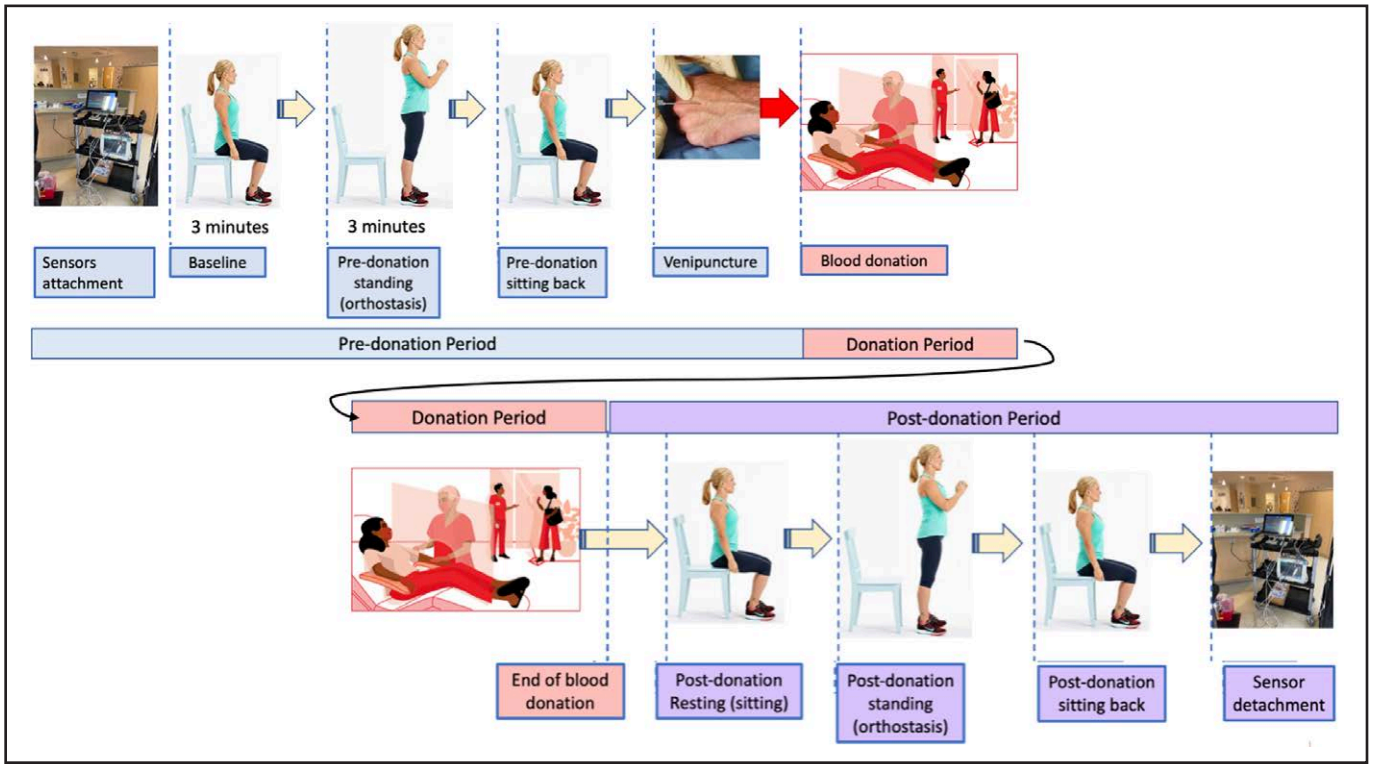

Figure 2. The schematic diagram of the controlled hemorrhage protocol before, during, and after the blood donation.

TABLE 1.

List of Physiologic Features Computed From the Dataset

Data Source (Type)	Feature Category	Feature Name	Remarks
Electrocardiography (waveform, 250 Hz)	Heart rate variability (time domain)	Root mean square SD (ms)	20 s median
		SD of N-to-N interval (ms)	20 s median
		SD of subsequent (ms^2)	20 s median
		Percentage of successive RR intervals that differ by more than 50 ms	20 s median
		Percentage of successive RR intervals that differ by more than 20 ms	20 s median
	Heart rate variability (time domain, nonlinear)	Sample entropy	120 s median
	Heart rate variability (frequency domain)	LF power (ms^2)	0.04–0.15 Hz
		HF (ms^2)	0.15–0.4 Hz
		LF/HF ratio	
Respiratory waveform (250 Hz)	RR	RR	20 s median
PPG, waveform (125 Hz)	Morphologic analysis (raw wave)	PPG amplitude	Beat-to-beat
		Plethysmography amplitude variation	20 s median
		Time to peak unit: ms	Time from trough to the next peak
		Slope	Angle from the trough to the next peak
	Morphologic analysis (second derivatives)	Peripheral vascular resistance	A3/(A1+A2) with the area under the curve of the PPG
		Stress-induced vascular response	(A2+A3)/A1
Continuous noninvasive arterial pressure monitoring device (waveform and numerical (100 Hz)	Numerical analysis	Systolic, diastolic, and mean arterial pressures	20 s median
		Cardiac output and cardiac index	20 s median

HF = high frequency power, LF = low frequency, PPG = photoplethysmography, RR = respiratory rate.

density signal providing partial information on blood volume, flow, and respiratory oscillation as well as sympathetic activity (14). All PPG waveforms were processed using bandpass filters as described above. Then the rule of skewness was applied to determine morphologically usable waveform (15). The PPG signals were analyzed to produce variables using a 30-second time period, with 10-second overlapping windows. Morphologic variables included the amplitude of the peak from the trough (plethysmography amplitude), peak-to-peak time, trough-to-peak time, and slope (from trough to next consecutive peak). The time-related variable was calculated by measuring the time between the peak of the preceding ECG R wave to the following consecutive PPG baseline immediately before the peak—called finger pulse arrival time, which was an approximation of the pulse transit time (16).

The finger cuff plethysmographic sensor (CNAP, CNS systems) was calibrated with the cuff sphygmomanometer, and continuous arterial pressure waveform data were collected into a LiDCO rapid device which reported beat-to-beat arterial pressure metrics (systolic, diastolic, mean, PP) and PP variation over 20 seconds as well as estimating stroke volume from the arterial pressure waveform. Collected waveform data were preprocessed with the Savitzky-Golay filter (17) to allow measurement of systolic and diastolic times.

Time Segmentation

All processed waveform variables were segmented as depicted in Figure 2, which divided the time series data based on different volume statuses and participants' positions before, during, and after bleeding. First, to define the steady-state effects of bleeding the prebleed resting step was compared with the postbleed resting step. Second, the prebleed resting step was compared with prebleed orthostasis defining the impact of orthostatic challenge before bleeding. Third, the postbleed resting step was compared with postbleed orthostasis to assess positional influence after bleeding. Fourth, prebleed and postbleed orthostasis were compared with each other to investigate the effect of blood loss on orthostatic challenge.

Statistical Methods

The median and interquartile ratio of all primary and featurized data were calculated for each time window. A nonparametric one-way analysis of variance test (Kruskal-Wallis) was conducted to investigate the difference between participants who experienced AE group and those who did not. The distribution of high-dimensional features between the AE and non-AE groups was conducted using the t-stochastic neighbor embedding (t-SNE), one of the unsupervised machine learning algorithms (18). All statistical and data-driven methods were performed using Matlab R2022b (The MathWorks, Natick, MA) and statistical packages in Python 3.11 (Python Software Foundation, Wilmington, DE).

RESULTS

Data Overview

We enrolled 55 healthy volunteers during blood donation. Two subjects were excluded due to difficulty with IV access, and two had inaccurate annotation information. As a result, ECG and PPG waveform-level data were available for 51 participants, and CNAP waveform data were available for 49 participants (**Supplementary Fig. 1**, http://links.lww.com/CCX/B326).

The 51 participants had an average age of 49.4 years, were 54.9% male, 96% White, and an average body mass index 27.2. The average prebleed physiologic data were BP 125/75 mm Hg, mean arterial pressure was 92 mm Hg, and hemoglobin 14.3 g/dL. On average, 494.5 mL of blood was donated over 7 minutes and 3 seconds, at a speed of 0.95 mL/kg/min. Assuming the blood content was approximately 5 L in a 70-kg individual, the percentage of blood loss over the blood volume was estimated at around 7–8%. Overall, the volume loss over time for all participants was linear (**Supplementary Fig. 2**, http://links.lww.com/CCX/B326). Fifteen participants (29%) have hypertension and on antihypertensive medications. Twenty-two participants (43.1%) participants have history of smoking (current or former). Six of 51 participants (11.8%) reported AE, such as nausea (n = 4), lightheadedness (n = 5), dizziness (n = 4), observed facial flushes (n = 2), hyperventilation (n = 1), or impending doom (n = 1) during the postbleed orthostatic maneuver period. Clinical descriptive characteristics were outlined (**Supplementary Table 1**, http://links.lww.com/CCX/B326).

We saw no significant changes in mean arterial pressure, PP, or cardiac output during bleeding or comparing prebleed to postbleed intervals (**Supplementary Fig. 3**, http://links.lww.com/CCX/B326).

Feature Changes Reflecting Prebleed and Postbleed Resting Periods and Orthostatic Challenges

When the two resting periods prebleed and postbleed were compared, features were not significantly different except for the decreased acceleration time. However, when the baseline (prebleed) resting period was compared to its baseline orthostatic challenge, increased HR, decreased HRV time domain (pNN20), and a set of PPG-derived morphologic feature changes (decreased PA and increased plethysmography amplitude variation [PAV]) were observed. The postbleed orthostatic challenge demonstrated greater changes in HRV time-domain features (decreased RMSSD, SDNN, SDSD, pNN20, and pNN50) and a frequency-domain feature (decreased HF) compared with the prebleed orthostatic challenge. However, a few feature behaviors including increased HR and PAV, decreased PA, and increased PAV were similar to prebleed orthostatic challenge. Interestingly, when the two orthostatic periods (prebleed and postbleed) were compared with each other independent of their baselines, although HR increased more postbleed, feature behavior changes were similar (decreased HRV time-domain features and decreased HF, along with increased HR, decreased PA, and increased PAV). Features with significant differences related to both bleeding and/or AE are summarized in **Table 2**.

Feature Changes Over Time During Bleeding

The prebleed resting baseline features were compared with those at every 100 mL of blood loss during bleed. Overall, HRV time-domain features demonstrated the most sensitive changes from the initial 100 mL blood loss (SDNN) and persisted throughout the entire bleeding course to 500 mL blood loss. From 300 mL blood loss onward, decreased HRV time-domain features (SDNN, RMSSD, and SDSD) and increased HRV frequency-domain feature (LF) were seen. Above 400 mL blood loss, decreased acceleration time was seen (**Fig. 3**).

Clinical and Physiologic Characteristics of "Adverse Event" Group

AE was observed and documented in 6 participants, all during the postdonation orthostatic challenge, and lasted for 3-15 minutes. The AE group was younger (37.7 yr AE vs. 50.9 yr non-AE, $p < 0.005$), and more likely to be female (83.3% female AE vs. 40% female non-AE, $p < 0.001$). The AE group also demonstrated a significant decrease in SampEn at the postbleed orthostatic challenge as compared with the non-AE group ($p = 0.003$) (**Fig. 4**). Notably, the AE group had an increased history of joint hypermobility (66.7% vs. 6.7% in the non-AE group, $p < 0.001$), defined as greater than 2 points of Beighton's score (**Supplementary Table 2** http://links.lww.com/CCX/B326). Other clinical characteristics showed no statistically significant difference. When complexs feature differences were graphically displayed onto the lower dimensional space using the t-SNE algorithm, there were no discernible physiologic feature differences between AE and non-AE groups overall. When segmented into different position and volume changes, there were no significant changes except for the postbleed orthostatic stage when some of the AE group was differently mapped (**Supplementary Fig. 4**, http://links.lww.com/CCX/B326).

DISCUSSION

We demonstrated that the physiologic vital sign signatures and their features from various waveforms could identify rapid bleeding in healthy blood donors with as little as 100 mL of blood loss. We are unaware of any similar efforts to investigate early physiologic signatures of hemorrhagic events in conscious healthy humans. Intraoperative studies of the impact of exchange transfusion on hemodynamics used small aliquots of blood per step and did not analyze hemodynamic features or used dynamic measures to assess cardiovascular state. Also, unlike recent human models (19, 20), our participants were bled without mechanical ventilatory support. Thus, our model better reflected signatures of acute bleeding outside of the operating room. Our findings may not only enlighten our understanding of the intricate physiologic compensation seen during the early stage of severe hemorrhage but also help to inform the development of data-driven decision-support models to detect or even predict such early changes. Consistent with ATLS teaching, we also

TABLE 2.

Features With Statistically Significant ($p < 0.05$) Changes During the Experiment ($n = 51$)

Feature Types	Prebleeding Sitting Vs. Prebleeding Standing (No Interval Volume Differences, Orthostatic Change)	Prebleeding Sitting Vs. Postbleeding Sitting (interval Volume Differences, Same Position)	Postbleeding Sitting Vs. Postbleeding Standing (No Interval Volume Differences, Orthostatic Change)	Prebleeding Standing Vs. Postbleeding Standing (Interval Volume Differences, Same Position)	Difference Between Prebleeding Sitting to Standing to Postbleeding Sitting to Standing
Heart rate	HR (↑)		HR (↑)	HR (↑)	HR (↑)
Heart rate variability (time domain)	pNN20 (↓)		RMSSD (↓↓) SDNN (↓) SDSD (↓↓) pNN20 (↓) pNN50 (↓)	RMSSD (↓↓) SDNN (↓) SDSD (↓↓) pNN20 (↓) pNN50 (↓)	
Heart rate variability (frequency-domain)			HF (↓)	HF (↓)	
Plethysmography values	PA (↓) PAV (↑)	Acceleration (↓)	Acceleration (↓) PA (↓) PAV (↑)	Acceleration (↓) PA (↓) PAV (↑)	PA (↓↓)

HF = high frequency, PA = plethysmography amplitude, PAV = plethysmography amplitude variation, pNN20 = the percentage of total consecutive heart rate variability values with difference ≥ 20 ms, RMSSD = root mean square SD, SDNN = SD of N-to-N interval, SDSD = SD of successive differences.

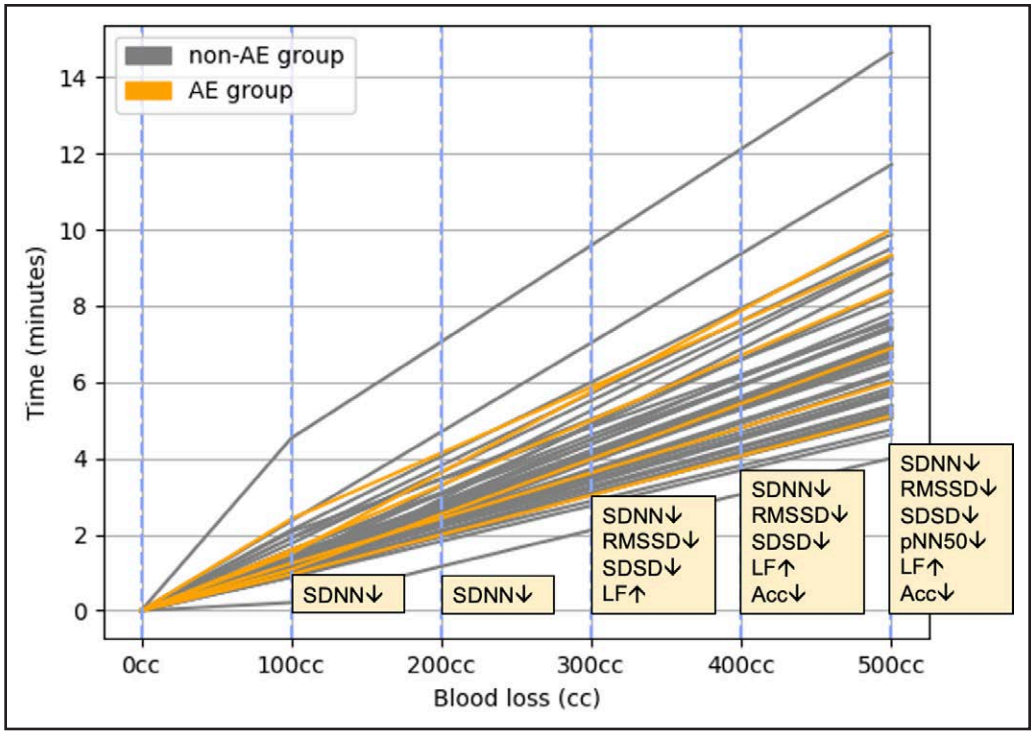

Figure 3. Statistically significant ($p < 0.05$) feature changes across all subjects ($n = 51$) during the blood donation period. All features were compared with the prebleeding baseline features. Heart rate variability time-domain features were found to be very sensitive to the bleeding, with its appearance from 100 cm^3 of bleeding. Acc = acceleration of the photoplethysmography waveform, LF = low frequency, RMSSD = root mean square of the SD, SDNN = SD of the interbeat interval, SDSD = SD of successive differences.

saw no changes in arterial pressure or cardiac output during bleeding. Thus, to identify rapid bleeding early, one needs featurization of these vital signs.

Feature Changes Over Time in Previous Animal Models

In an animal model, Scully et al examined physiologic compensatory mechanisms in Merino Sheep (n = 8) during hemorrhage at either slow (0.25ml/kg/min) and fast (1.25ml/kg/min) bleeding. According to their analysis, the speed of bleeding did not make a difference in the pattern of compensatory response and its loss at the end of the bleeding, until MAP decreased steeply (21). We previously showed in a porcine acute bleeding model that early bleed detection was better if using invasive monitoring (such as arterial and pulmonary arterial catheters) and higher sampling rates compared with noninvasive monitoring and lower sampling rates. We also demonstrated that early identification of blood loss could be greatly improved if a subject-specific baseline data set were used to define normal (22, 23). Regrettably, in trauma and other emergently bleeding conditions, such stable baseline data are lacking.

The Physiologic Feature Behaviors Before, During, and After the Blood Donation

Across all of our study participants, regardless of volume status, many physiologic features including HRV time and frequency domains as well as PPG-derived features changed when the participants' positions were changed from sitting to standing (i.e. orthostatic challenge). All five HRV time-domain features as well as HF in the frequency domain were decreased with orthostasis after bleed, or comparing two orthostatic periods before and after bleed. Decreased RMSSD is a known risk factor for sudden death in the epilepsy population (24), associated with decreased parasympathetic involvement suggesting stressful conditions. Likewise, decreased HF region implies increased stress with disruption of normal respiratory sinus arrhythmias (25). Decreased PPG amplitude and increased PPG amplitude variation are linked with blood loss in ventilated patients at 10% of blood volume loss (20), or in the operating room to identify fluid-responsiveness (19). We did not observe such changes when the two resting or orthostatic positions were compared. These findings suggested that dynamic hemodynamic signals reflect hemodynamic derangement during a relatively small amount of blood loss or position changes, although physiologically well-managed.

During the bleeding period, our findings indicated the occurrence of a gradual physiologic compensation correlating with progressive blood loss. At the very early course of bleeding (100 mL), a decrease in SDNN was observed, which is known to be one of the most sensitive short-term HRV features along with

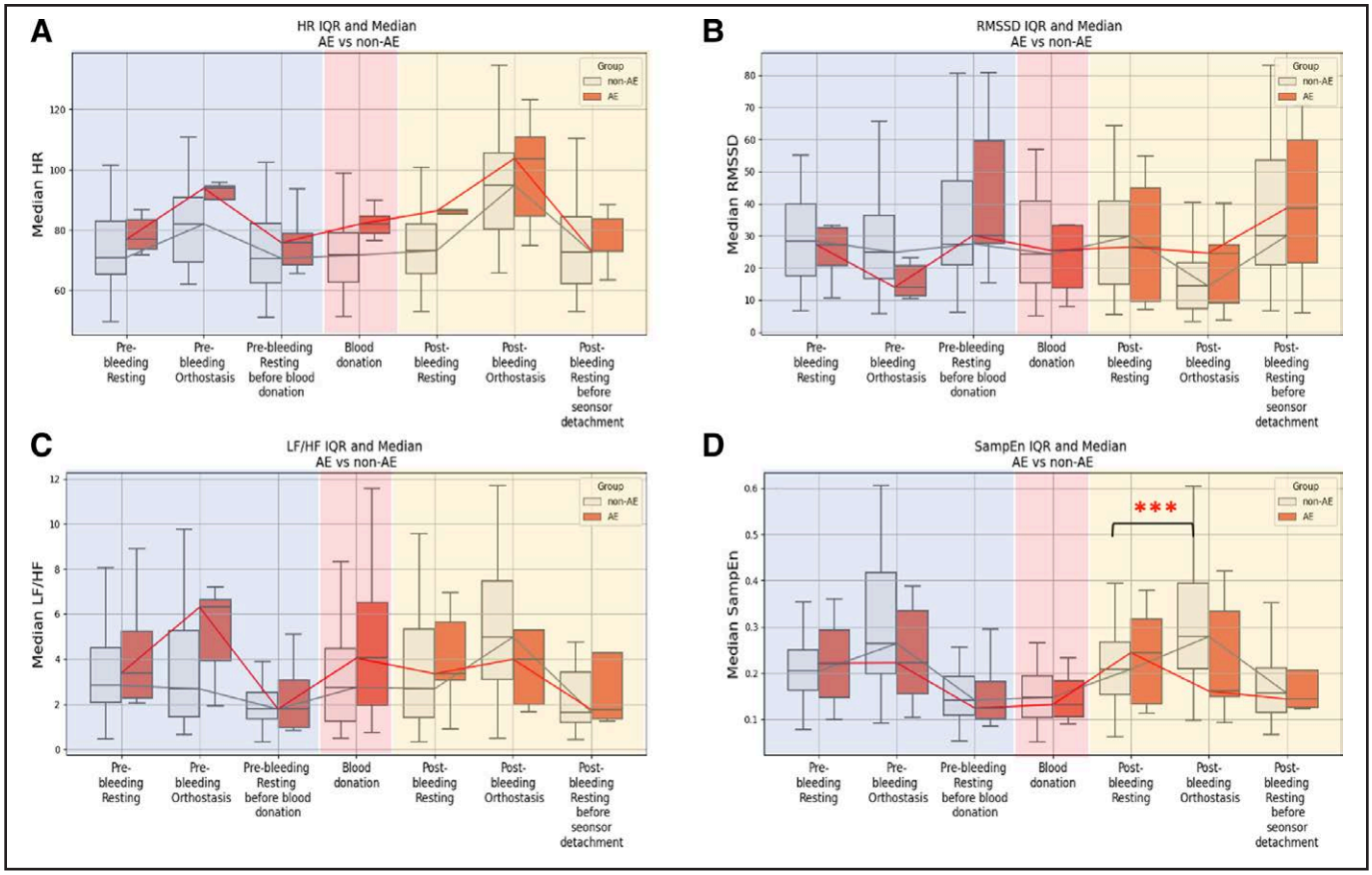

Figure 4. Median and interquartile ranges (IQRs) for heart rate (HR) and HR variability (HRV) features through the course of blood donation. The *blue-shaded* area denotes the prehemorrhage donation period, and the *red* and *yellow shades* represent blood donation and postblood donation, respectively. **A**, HR; **B**, an example of HRV time-domain feature (root mean square of SD [RMSSD]); **C**, an example of HRV frequency-domain feature (low-frequency [LF] to high-frequency [HF] ratio); **D**, HRV nonlinear feature—sample entropy (SampEn). Adverse event (AE) indicates a group of subjects experienced AEs after the blood donation. Non-AE denotes a group of subjects without such AEs. In the AE group, the SampEn decreased with orthostasis after the blood loss, whereas the SampEn in the non-AE group slightly increased ($p = 0.003$).

RMSSD even with a short signal length (26). From 300 mL of bleeding, other HRV time-domain features became significant, which was anticipated given the decrease in HRV is closely related to increased sympathetic response and preload insufficiency. A transient increase in LF was also observed, implying a temporary enhancement in sympathetic tone, which dissipated quickly after the bleeding was completed. However, this LF increase is a mixture of sympathetic and parasympathetic actions, making it challenging to interpret (27, 28). Nevertheless, the consistent presence of such differences up to 500 mL of blood loss indicated that the dynamic feature behavior of the earliest signatures of bleeding appeared to be far ahead of clinically recognizable blood loss (6), or previously observed early physiologic variables from an animal study (29).

Distinctive Characteristics of Adverse Events

All of our AE occurred during orthostasis after blood donation. From previous studies, known risk factors for AE events after blood donation include younger age, female, first-time blood donor, and lower body weight (30), which was also demonstrated in our participants. Of note, the AE rate was higher (11.8%) in our study than described in the literature (1-5%). This high rate was likely due to the postbleed orthostasis stage in our study protocol being much earlier (after 3 min of resting) than standard postbleed resting and standing up (usually 10-min rest in a donation chair). The relatively short postbleed resting time before standing up would limit the time for fluid recruitment from extravascular to the intravascular space.

Decreased sample entropy upon orthostasis after bleed was the only distinctive feature for the AE group in our study. Decreased sample entropy is known to reflect cardiovascular instability through nonlinear HRV metric and is found to be a useful feature to predict the necessity of the life-sustaining intervention in a real-life scenario (31, 32) or to risk-stratify more vulnerable donors for blood donation to minimize postdonation AEs.

The t-SNE analysis did not reveal remarkable differences among the AE and non-AE groups. This could be due to the combination of high-dimensional features masked characteristic feature behaviors when presented in a low-dimensional space (33). Our analysis suggested that high-dimensional combinations of features across all positions or volume changes did not sufficiently discriminate the AE from the non-AE group.

Toward Building a Decision-Support System

The early identification of bleeding events is not only physiologically intriguing but also desirable in the clinical setting, as it could potentially lead to an earlier warning and application of mitigating interventions (34). Because a patient can lose 1000 mL (approximately 20% of total blood) in 15 min in a major bleeding event, a decision-support model alarm should be available no later than 5-6 minutes into the bleeding episode, leaving at least 10 minutes of response time for clinicians to treat patients before serious organ hypoperfusion occurs. With an average of 7 minutes of bleeding time, our human bleeding protocol could be a good starting point to build a data-driven model for the early detection of hemorrhage. We previously demonstrated good performance of a ML-derived early bleeding detection in our porcine model (29) but has not been analyzed in a controlled fashion in human. Our current analysis could be leveraged to identify high-risk blood donation volunteers, peripartum patients, and postoperative subjects, or triage management priorities in an emergent situation.

Limitations

Our study had several limitations. The study was designed as a single-center observational study. However, we had two different sites (1 suburban and 1 urban) where patient demographics were slightly different. Also, this was a prospectively conducted study in a controlled setting. The sample size was set as 55 with actual recruitment of 51 in ECG and PPG data. Yet, although modest, this represented the largest cohort among animal or human bleeding protocol published to date. We are currently planning to perform a larger human-controlled hemorrhage analysis in the blood donation setting. Our measurements included only noninvasive physiologic signatures, and the noninvasive parameters could be less accurate than invasive measurements, comparable to our previous works (22, 23). Lastly, although various clinical decision-support model could be developed using larger population, current study design of constant rate of bleeding with blood donation may not be easily generalized as the variable rates of hemorrhage in different clinical settings.

CONCLUSIONS

In a continuous vital sign collection from healthy volunteers donating blood, various abnormal sympathetic response patterns were observed in individuals experiencing AEs during and after blood donation. Early physiologic changes during blood loss (as early as 100 mL) could be identified in noninvasive vital sign features. Decreased sample entropy during postbleed orthostasis was a discriminating feature of participants experiencing AEs. Continuous featurization of physiologic variables during blood loss could lead to earlier detection and intervention.

ACKNOWLEDGMENTS

The authors thank the Vitalant Blood Donation Center (medical director, Dr. Joseph Kiss, Division of Hematology and Oncology, University of Pittsburgh) for allowing us to perform our study.

1 *Division of Pulmonary, Allergy, and Critical Care Medicine, Department of Medicine, School of Medicine, University of Pittsburgh, Pittsburgh, PA.*

2 *Acute and Tertiary Care, School of Nursing, University of Pittsburgh, Pittsburgh, PA.*

3 *Department of Critical Care Medicine, School of Medicine, University of Pittsburgh, Pittsburgh, PA.*

Supplemental digital content is available for this article. Direct URL citations appear in the printed text and are provided in the HTML and PDF versions of this article on the journal's website (http://journals.lww.com/ccejournal).

The research was conducted with the National Institutes of Health (NIH) K23 funding (grant K23GM138984, Dr. Yoon).

The remaining authors have disclosed that they do not have any potential conflicts of interest.

For information regarding this article, E-mail: yoonjh@upmc.edu

REFERENCES

1. Owattanapanich N, Chittawatanarat K, Benyakorn T, et al: Risks and benefits of hypotensive resuscitation in patients with traumatic hemorrhagic shock: A meta-analysis. *Scand J Trauma Resusc Emerg Med* 2018; 26:107
2. Centers for Disease Control and Prevention: Fatal injury and violence data. 2022. Available at: https://www.cdc.gov/injury/wisqars/fatal.html. Accessed August 24, 2022
3. Stewart RM, Myers JG, Dent DL, et al: Seven hundred fifty-three consecutive deaths in a level I trauma center: The argument for injury prevention. *J Trauma* 2003; 54:66–70; discussion 70
4. Teixeira PG, Inaba K, Hadjizacharia P, et al: Preventable or potentially preventable mortality at a mature trauma center. *J Trauma* 2007; 63:1338–46; discussion 1346
5. Guyton AC, Coleman TG, Granger HJ: Circulation: Overall regulation. *Annu Rev Physiol* 1972; 34:13–46
6. Mutschler M, Paffrath T, Wölfl C, et al: The ATLS® classification of hypovolaemic shock: A well established teaching tool on the edge? *Injury* 2014; 45:S35–S38
7. Mutschler M, Nienaber U, Brockamp T, et al; TraumaRegister DGU: A critical reappraisal of the ATLS classification of hypovolaemic shock: Does it really reflect clinical reality? *Resuscitation* 2013; 84:309–313
8. Guly HR, Bouamra O, Little R, et al: Testing the validity of the ATLS classification of hypovolaemic shock. *Resuscitation* 2010; 81:1142–1147
9. Malek S, Reinhold EJ, Pearce GS: The Beighton score as a measure of generalised joint hypermobility. *Rheumatol Int* 2021; 41:1707–1716
10. Buendía-Fuentes F, Arnau-Vives MA, Arnau-Vives A, et al: High-bandpass filters in electrocardiography: Source of error in the interpretation of the ST segment. *ISRN Cardiol* 2012; 2012:706217
11. Xie CM, McCullum L, Johnson A, et al: Waveform Database Software Package (WFDB) for Python (version 3.4.1). PhysioNet 2021. doi: 10.13026/egpf-2788
12. Heart rate variability: Standards of measurement, physiological interpretation and clinical use. Task Force of the European Society of Cardiology and the North American Society of Pacing and Electrophysiology. *Circulation* 1996; 93:1043–1065. doi: 10.1161/01.CIR.93.5.1043
13. Richman JS, Moorman JR: Physiological time-series analysis using approximate entropy and sample entropy. *Am J Physiol Heart Circ Physiol* 2000; 278:H2039–H2049
14. Allen J: Photoplethysmography and its application in clinical physiological measurement. *Physiol Meas* 2007; 28:R1–39
15. Elgendi M, Meo M, Abbott D: Optimal signal quality index for photoplethysmogram signals. *Bioengineering (Basel)* 2016; 3:26
16. Block RC, Yavarimanesh M, Natarajan K, et al: Conventional pulse transit times as markers of blood pressure changes in humans. *Sci Rep* 2020; 10:16373
17. Press WH, Teukolsky SA: Savitzky-Golay smoothing filters. *Comput Phys* 1990; 4:669
18. van der Maaten L HG: Visualizing data using t-SNE. *J Mach Learn Res* 2008; 9:2579–2605
19. Cannesson M, Attof Y, Rosamel P, et al: Respiratory variations in pulse oximetry plethysmographic waveform amplitude to predict fluid responsiveness in the operating room. *Anesthesiology* 2007; 106:1105–1111
20. Shamir M, Eidelman LA, Floman Y, et al: Pulse oximetry plethysmographic waveform during changes in blood volume. *Br J Anaesth* 1999; 82:178–181
21. Scully CG, Daluwatte C, Marques NR, et al: Effect of hemorrhage rate on early hemodynamic responses in conscious sheep. *Physiol Rep* 2016; 4:e12739
22. Wertz A, Holder AL, Clermont G, et al: Increasing cardiovascular data sampling frequency and referencing it to baseline improve hemorrhage detection. *Crit Care Explor* 2019; 1:e0058
23. Pinsky MR, Wertz A, Clermont G, et al: Parsimony of hemodynamic monitoring sufficient for detection of hemorrhage. *Anal Anesth* 2020; 130:1176–1187
24. DiGiorgio CM, Miller P, Meymandi S, et al: RMSSD, a measure of vagus-mediated heart rate variability, is associated with risk factors for SUDEP: The SUDEP-7 inventory. *Epilepsy Behav* 2010; 19:78–81
25. Jönsson P: Respiratory sinus arrhythmia as a function of state anxiety in healthy individuals. *Int J Psychophysiol* 2007; 63:48–54
26. Munoz ML, van Roon A, Riese H, et al: Validity of (ultra-)short recordings for heart rate variability measurements. *PLoS One* 2015; 10:e0138921
27. von Rosenberg W, Chanwimalueang T, Adjei T, et al: Resolving ambiguities in the LF/HF ratio: LF-HF scatter plots for the categorization of mental and physical stress from HRV. *Front Physiol* 2017; 8:360
28. Houle MS, Billman GE: Low-frequency component of the heart rate variability spectrum: A poor marker of sympathetic activity. *Am J Physiol* 1999; 276:H215–H223
29. Chen Y, Yoon JH, Pinsky MR, et al: Development of hemorrhage identification model using noninvasive vital signs. *Physiol Meas* 2020; 41:055010
30. Trouern-Trend JJ, Cable RG, Badon SJ, et al: A case-controlled multicenter study of vasovagal reactions in blood donors: Influence of sex, age, donation status, weight, blood pressure, and pulse. *Transfusion* 1999; 39:316–320
31. Rickards CA, Ryan KL, Convertino VA: Characterization of common measures of heart period variability in healthy human subjects: Implications for patient monitoring. *J Clin Monit Comput* 2010; 24:61–70
32. Peev MP, Naraghi L, Chang Y, et al: Real-time sample entropy predicts life-saving interventions after the Boston Marathon bombing. *J Crit Care* 2013; 28:1109.e1–1109.e4
33. Cai TT, Ma R: Theoretical foundations of t-SNE for visualizing high-dimensional clustered data. *J Mach Learn Resc* 2022; 23:13581–13634
34. Yoon JH, Pinsky MR: Predicting adverse hemodynamic events in critically ill patients. *Curr Opin Crit Care* 2018; 24:196–203